Hyunpyo Shin
Graduate School of Mechanical and Aerospace Engineering,
Seoul National University,
Seoul 151-742, South Korea

Sungchul Lee
Korean Institute of Machinery and Materials,
Daejeon 305-343, South Korea

Woosung In
Graduate School of Mechanical and Aerospace Engineering,
Seoul National University,
Seoul 151-742, South Korea

Jay I. Jeong[1]
School of Mechanical and Automotive Engineering,
Kookmin University,
861-1, Jeongnung-Dong,
Seungbuk-Gu, Seoul, South Korea
e-mail: jayjeong@kookmin.ac.kr

Jongwon Kim
School of Mechanical and Aerospace Engineering,
Seoul National University,
Seoul, South Korea

Kinematic Optimization of a Redundantly Actuated Parallel Mechanism for Maximizing Stiffness and Workspace Using Taguchi Method

We present an optimization procedure that uses the Taguchi method to maximize the mean stiffness and workspace of a redundantly actuated parallel mechanism at the same time. The Taguchi method is used to separate the more influential and controllable variables from the less influential ones among kinematic parameters in workspace analysis and stiffness analysis. In the first stage of optimization, the number of experimental variables is reduced by the response analysis. Quasi-optimal kinematic parameter group is obtained in the second stage of optimization after the response analysis. As a validation of the suggested procedure, the kinematic parameters of a planar 2-DOF parallel manipulator are optimized, which optimization procedure is used to investigate the optimal kinematic parameter groups between the length of the link and the stiffness.
[DOI: 10.1115/1.4002268]

1 Introduction

Recently, redundantly actuated parallel mechanisms have been studied because of their advantages such as no actuator singularities [1], which allows more workspace and additional stiffness, which is generated by the internal preload assignment [2]. The stiffness is enhanced by assigning an internal torque distribution among the actuating joints and, therefore, is dependent on the number of additional actuators [3].

The stiffness and workspace of the mechanism are important design factors of a redundantly actuated parallel mechanism. For example, haptic devices usually require a software routine to control their stiffness and also a large workspace at the same time [4–6]. These two factors are also related to each other, and the stiffness is expected to increase by the kinematic parameter optimization. Xu and Li [7] used the particle swarm optimization method in the stiffness optimization of a 3-DOF parallel kinematic machine. Xu and Li [8] also investigated the stiffness of a 3-DOF translational parallel manipulator by screw theory and discussed the influences of the change in kinematic parameters on the stiffness of the manipulator. Lee et al. [9] used the composite design index to optimize the workspace of a five-bar redundantly actuated system. Thus, in the design process of a redundantly actuated parallel mechanism, we should consider how much active stiffness can be guaranteed by assigning an internal torque distribution. At the same time, the workspace of the mechanism should be maximized. However, the relationship between the workspace and stiffness is contrary to each other according to previous researches [10,11].

In this study, the stiffness and the workspace of a planar two degrees of freedom (2-DOF) parallel manipulator are optimized. The mechanism, that is, the manipulator, has three actuators although it needs only two actuators for control. Thus, the one additional actuator is used to control the stiffness of the mechanism [3].

The Taguchi method, whose procedure is depicted in Fig. 1, was introduced in order to conduct the optimization. This method was originally developed for quality engineering and is a tool for systematically optimizing a given criterion by experiments or simulations [12].

For our problem, a stiffness matrix, which is expressed as a Hessian matrix is used. The Hessian matrix has three dimensional elements obtained from the derivative of the Jacobian matrix and it exists in case of redundant actuation situation. To examine the relationship between kinematic parameters and stiffness, partial differentiation of the Hessian matrix needs to be performed with respect to the kinematic parameters for the given mechanism. Moreover, additional Jacobian operation is also required to obtain the matrix since the dimension of the Hessian matrix is already three. As a result, complexity should be increased in proportion to the number of kinematic parameters and dimension.

Instead of formulating a numerical procedure, here, we optimized the workspace and mean stiffness by using the Taguchi, which is easy to apply. Compared with the analytic approach, the Taguchi method requires only the output response from the input and feedback without increasing the dimension of the matrix. Especially, the numerical approach for optimization is not appropriate for early stages of design because of heavy numerical cost.

The Taguchi method for design of experiments was conducted by several previous researchers. Lee et al. [12] used the Taguchi method to size the actuators of a 6-DOF parallel mechanism. Lee and Kim [13] used the Taguchi method in proportional-integral-derivative (PID) controller gain tuning of a 6-DOF parallel

[1]Corresponding author.

Contributed by the Engineering Division of ASME for publication in the JOURNAL OF COMPUTATIONAL AND NONLINEAR DYNAMICS. Manuscript received June 14, 2009; final manuscript received December 17, 2009; published online October 11, 2010. Assoc. Editor: Nobuyuki Shimizu.

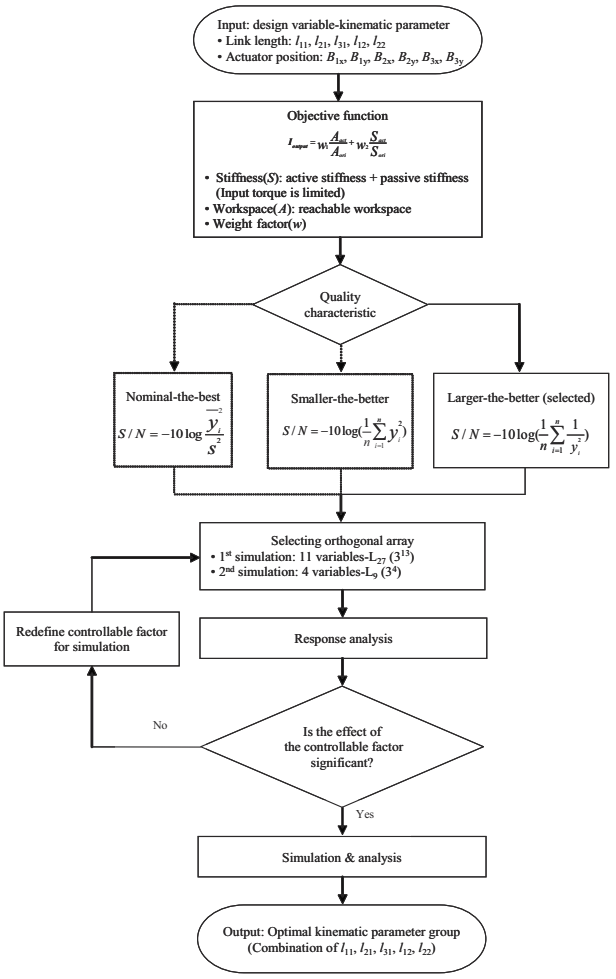

Fig. 1 Optimization procedure in Taguchi method

mechanism. Rout and Mittal [14] used the analysis of variance (ANOVA) technique to find the parameter set that can minimize the mean positional error of a 2-DOF revolute-revolute (RR) planar manipulator.

Herein, we used the Taguchi method to examine the relationship of the kinematic parameters and to obtain quasi-optimal solution of a 2-DOF parallel manipulator to ensure the maximum mean stiffness while considering workspace simultaneously.

The related research on the performance of parallel mechanisms in view of wrench capability analysis has been done. Garg et al. [15] studied the maximum applicable force and associated moment of 3–revolute-revolute-revolute-spherical (3-RRRS) redundantly actuated parallel mechanism in various positions. Nokleby et al. [16] showed the improvement of force capability in redundant actuation by using scaling factor method. They used maximum and minimum values of performance index.

The objective of this study mainly focuses on the examination of the change of the mean stiffness and the workspace with respect to the change in the kinematic parameters of the mechanism and focuses on extracting dominant kinematic parameters that influence stiffness and workspace of the given mechanism. We used mean value of stiffness by averaging stiffness in total workspace, which includes active stiffness and passive stiffness at given positions of the mechanism.

The response analysis of the Taguchi method was conducted to reduce the number of experimental variables, that is, eleven controllable factors to the four most influential factors. The L_{27} (3^{13}) orthogonal array was used to reduce the time spent in the first simulation process. After conducting the response analysis, the L_9 (3^4) orthogonal array was applied with the selected four controllable factors. Through the optimization procedures, we found several kinds of optimal kinematic parameter level groups. From the results, we derived the relationship between the various link lengths and the change in workspace and mean stiffness of the planar 2-DOF parallel manipulator.

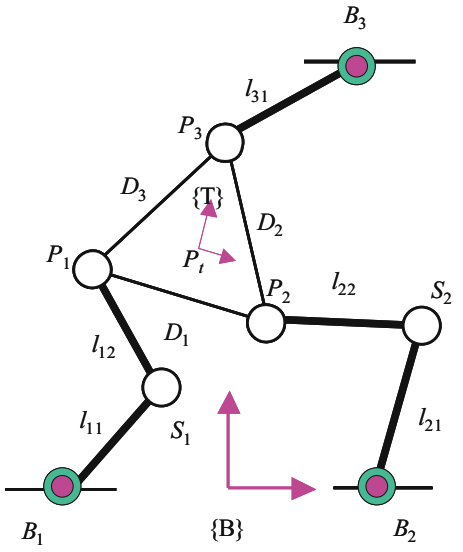

Fig. 2 Schematic diagram of the planar 2-DOF parallel manipulator

2 Kinematic and Jacobian Analysis

In our research, we used a planar 2-DOF parallel manipulator [3,17] consisting of five links l_{ij} and a tool plate. It also has eight revolute joints, namely, three ground joints B, two intermediate joints S_i, and three tool plate joints P. The mechanism has two kinematic degrees of freedom and three joints that are actuated. A schematic diagram of the planar 2-DOF parallel manipulator is depicted in Fig. 2.

Constraint and forward Jacobian are the relationships between the time derivatives of the input variables and output variables of the kinematic expressions of the constraint equation and forward equation, respectively. q_{all} represents the total joint vector. q_u is an angular position vector of independent joints. q_v is an angular position vector of dependent joints. q_r is an angular position vector of actuation joints. A total of eight joints exist in the planar 2-DOF parallel manipulator. However, the last three joints do not appear in the q_{all} joint vector because they are used as a constraint condition in the kinematic analysis.

$$q_{all} \equiv [q_1, q_2, q_3, q_4, q_5]^T$$

$$q_{all} = U \begin{bmatrix} q_u \\ q_v \end{bmatrix} \tag{1}$$

$$U \in \Re^{5\times5}, \quad q_u \in \Re^{2\times1}, \quad q_v \in \Re^{3\times1}$$

$$q_r = V q_{all} \tag{2}$$

$$V \in \Re^{3\times5}, \quad q_r \in \Re^{3\times1} \tag{3}$$

where U is a relocation matrix, which rearranges the order of the independent and the dependent joint vector. V is a selection matrix, which chooses the actuating joint vector among the q_{all} vectors. The matrix U and V are obtained from below relationships, Eqs. (4) and (5).

$$q_{\text{all}} = U[q_u q_v]^T, \quad \begin{bmatrix} \theta_1 \\ \theta_2 \\ \theta_3 \\ \theta_4 \\ \theta_5 \end{bmatrix} = U \begin{bmatrix} \theta_1 \\ \theta_2 \\ \theta_3 \\ \theta_4 \\ \theta_5 \end{bmatrix}$$

$$U = \begin{bmatrix} 1 & 0 & 0 & 0 & 0 \\ 0 & 1 & 0 & 0 & 0 \\ 0 & 0 & 1 & 0 & 0 \\ 0 & 0 & 0 & 1 & 0 \\ 0 & 0 & 0 & 0 & 1 \end{bmatrix} \in \Re^{5\times 5} \tag{4}$$

$$q_r = V q_{\text{all}}, \quad \begin{bmatrix} \theta_1 \\ \theta_2 \\ \theta_3 \end{bmatrix} = V \begin{bmatrix} \theta_1 \\ \theta_2 \\ \theta_3 \\ \theta_4 \\ \theta_5 \end{bmatrix}, \quad V = \begin{bmatrix} 1 & 0 & 0 & 0 & 0 \\ 0 & 1 & 0 & 0 & 0 \\ 0 & 0 & 1 & 0 & 0 \end{bmatrix} \in \Re^{3\times 5} \tag{5}$$

The constraint Jacobian (7) is obtained by the time derivative of the geometric constraint Eq. (6). P_i is platform revolute joint and is showed in Fig. 2. It defines the relationship between independent joint q_u and dependent joint q_v.

$$g(q_{\text{all}}) = \begin{bmatrix} g_1 \\ g_2 \\ g_3 \end{bmatrix} = \begin{bmatrix} \|P_1 - P_2\|^2 - \|P_1^{\{T\}} - P_2^{\{T\}}\|^2 \\ \|P_2 - P_3\|^2 - \|P_2^{\{T\}} - P_3^{\{T\}}\|^2 \\ \|P_3 - P_1\|^2 - \|P_3^{\{T\}} - P_1^{\{T\}}\|^2 \end{bmatrix} = \begin{bmatrix} 0 \\ 0 \\ 0 \end{bmatrix}$$

$$g(q_{\text{all}}) = 0 \tag{6}$$

$$\frac{\partial g(q_{\text{all}})}{\partial t} = \frac{\partial g(q_{\text{all}})}{\partial q_{\text{all}}} \frac{\partial q_{\text{all}}}{\partial t} = G\dot{q}_{\text{all}} = 0 \tag{7}$$

We can find the relationship between the joint angles from the constraint equation as below.

$$\begin{bmatrix} G_u & G_v \end{bmatrix} \begin{bmatrix} \dot{q}_u \\ \dot{q}_v \end{bmatrix} = 0$$

$$\dot{q}_v = -G_v^{-1} G_u \dot{q}_u = \Phi \dot{q}_u \tag{8}$$

$$\dot{q}_r = \Gamma \dot{q}_u$$

$$\left(\text{define: } \Phi \equiv -G_v^{-1} G_u, \quad \Gamma \equiv VU \begin{bmatrix} I_{2\times 2} \\ \Phi \end{bmatrix} \right)$$

where Φ is Jacobian, which maps independent joints to dependent joints. Γ is Jacobian, which maps independent joints to actuation joints. These Jacobians will be used to perform stiffness analysis. Forward Jacobian is the relationship between the velocity of the independent joint and the velocity of the center of the tool platform.

$$\dot{x}_t = \frac{dx_t}{dt} = \frac{dx_t}{dq_{\text{all}}} \frac{dq_{\text{all}}}{dt} = J\dot{q}_{\text{all}}$$

$$J = \frac{dx_t}{dq_{\text{all}}} = \frac{1}{3} \frac{\partial (P_1 + P_2 + P_3)}{\partial q_{\text{all}}} \tag{9}$$

$$\dot{x}_t = J\dot{q}_{\text{all}} = JU \begin{bmatrix} \dot{q}_u \\ \dot{q}_v \end{bmatrix} = JU \begin{bmatrix} \dot{q}_u \\ \Phi \dot{q}_u \end{bmatrix} = JU \begin{bmatrix} I_{2\times 2} \\ \Phi \end{bmatrix} \dot{q}_u = J_f \dot{q}_u$$

$$\left(\text{define: } J_f = JU \begin{bmatrix} I_{2\times 2} \\ \Phi \end{bmatrix} \right) \tag{10}$$

The forward Jacobian matrix J_f of Eq. (10) can be used to obtain the relationship between the active joint torque τ_r and the exerted external forces f in the stiffness analysis.

3 Stiffness Analysis

Generally, the torque required to operate the parallel mechanism τ_u can be determined uniquely in nonredundant actuation [6]. However, in the case of redundant actuation, the torques τ_r of the actuators are not determined uniquely. The relationship between the independent joint torque τ_u and the actuated joint torque τ_r can be derived by the virtual work theorem. The relationship is presented in Eq. (12).

$$M\ddot{q}_u + C\dot{q}_u + N = \tau_u \tag{11}$$

$$\Gamma^T \tau_r = \tau_u \tag{12}$$

However, the actuating joint torque τ_r is not uniquely given but infinite numbers of the solutions can be derived since Γ^T does not have full rank.

$$\tau_r = (\Gamma^T)^+ \tau_u + (I_n - (\Gamma^T)^+ \Gamma^T) \varepsilon_n$$

$$\tau_{r,\text{motion}} = (\Gamma^T)^+ \tau_u$$

$$\tau_{r,\text{internal}} = (I_n - (\Gamma^T)^+ \Gamma^T) \varepsilon_n \tag{13}$$

where the actuating joint torque of a redundantly actuated parallel mechanism can be divided into two parts. The first term is the motion torque, which causes the motion of the mechanism. The second term is the internal preload torque, which does not induce any motion of the mechanism. Mathematically, the internal torque solution vector exists in the null space of the Jacobian. The internal preload torque can increase the active stiffness of a redundantly actuated parallel mechanism and is obtained from below relationships.

$$\Gamma^T \tau_r = \begin{bmatrix} 1 & 0 & \Phi_{11} \\ 0 & 1 & \Phi_{12} \end{bmatrix} \begin{bmatrix} \tau_1 \\ \tau_2 \\ \tau_3 \end{bmatrix} = \begin{bmatrix} 0 \\ 0 \end{bmatrix} \tag{14}$$

$$\tau_1 = -\Phi_{11} \tau_3$$

$$\tau_2 = -\Phi_{12} \tau_3 \tag{15}$$

The influence of internal preload torque is maximized when one actuator torque of three actuator torques reaches its limit torque output. Maximum torque output is applied in the next section of optimization procedure in the active stiffness term.

Stiffness can be defined as the ratio of the exerted force to an infinitesimal displacement, which is shown in Eq. (16).

$$K = \lim_{\Delta x_t \to 0} \frac{\Delta f}{\Delta x}_t = \frac{\partial f}{\partial x_t} \tag{16}$$

The relationship between the actuating joint torque of redundantly actuated parallel mechanisms and the force exerted on the platform of the mechanisms can be obtained by the virtual work theorem as in Eq. (17)

$$\tau_r^T dq_r = f^T dx_t$$

$$\tau_r^T \Gamma dq_u = f^T J_f dq_u$$

$$f = (\Gamma J_f^{-1})^T \tau_r = \Psi^T \tau_r$$

$$(\text{define: } \Psi \equiv \Gamma J_f^{-1}) \tag{17}$$

Hence, the stiffness of redundantly actuated parallel mechanisms can be represented by partial differentiation of Eq. (18). The relationship can be written as follows:

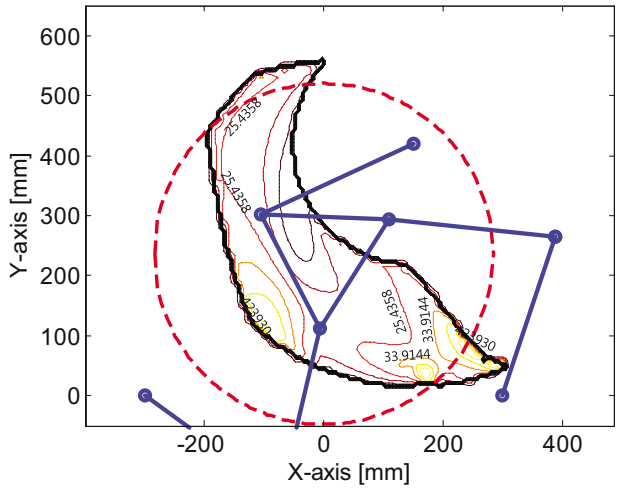

Fig. 3 Workspace and stiffness distribution of the planar 2-DOF parallel manipulator with original kinematic parameters when external force (1 N) is applied (l_{11}=280 mm, l_{21}=280 mm, l_{31}=280 mm, l_{12}=280 mm l_{22}=280 mm, workspace =0.108 m^2, mean stiffness=24.3864 N/m, and radius of gyration=0.568 m)

$$K = \frac{\partial \Psi^T \tau_r}{\partial x_t} = H^T \tau_r + \Psi^T \frac{\partial \tau_r}{\partial x_t} \tag{18}$$

where H is a Hessian matrix, which is the differential term of the Jacobian matrix.

The right side of Eq. (18) can be replaced by the relationship of Eq. (19),

$$\frac{\partial \tau_r}{\partial x_t} = \frac{\partial \tau_r}{\partial q_r}\frac{\partial q_r}{\partial x_t} = \frac{\partial \tau_r}{\partial q_r}\Psi \tag{19}$$

where $\partial \tau_r / \partial q_r$ is the torsional stiffness matrix (K_a) of each actuating joint, which is expressed as a diagonal matrix.

Finally, the Cartesian stiffness of redundantly actuated parallel mechanisms can be written as follows:

$$K = H^T \tau_r + \Psi^T K_a \Psi \tag{20}$$

In Eq. (20), the second term $\Psi^T K_a \Psi$ is the passive stiffness determined only by the position and orientation of the mechanism. However, the first term $H^T \tau_r$ represents the active stiffness. If we properly adjust the torque distribution τ_r with respect to the position and orientation of the mechanism, the total stiffness can be increased or decreased. The K_a is expressed in a diagonal matrix form and k_1, k_2, k_3 are constants.

$$K_a = \begin{bmatrix} k_1 & 0 & 0 \\ 0 & k_2 & 0 \\ 0 & 0 & k_3 \end{bmatrix} \tag{21}$$

Hessian matrix H can be obtained as below

$$H = \frac{\partial \Psi}{\partial x_c} = \left(\frac{\partial q_r}{\partial x_c}\right)^T \frac{\partial \Psi}{\partial q_r} = \Psi^T \frac{\partial (\Gamma J_f^{-1})}{\partial q_r} = \Psi^T \left(\frac{\partial \Gamma}{\partial q_r} J_f^{-1} + \Gamma \frac{\partial J_f^{-1}}{\partial q_r}\right) \tag{22}$$

where the forward Jacobian and constraint Jacobian, J_f and Γ, in Eq. (22) can be determined by joint values.

As an example of a stiffness analysis, Fig. 3 is illustrated. Figure 3 shows the workspace and the stiffness distribution of the planar 2-DOF parallel manipulator with the original kinematic parameters. The triangle and the connected lines constitute the kinematic structure of the manipulator. The contours and the numbers listed along the contours indicate the magnitude of the stiffness. The outermost contour displays the workspace of the manipulator, and the dotted circle is the radius of gyration (scaled down by half for convenience) to examine the distribution of the workspace.

Table 1 Typical S/N ratios

Objective	S/N ratio
Nominal-the-best	$S/N = -10 \log \bar{y}_i^2 / s^2$
Smaller-the-better	$S/N = -10 \log\left(\frac{1}{n}\Sigma_{i=1}^{n} y_i^2\right)$
Larger-the-better	$S/N = -10 \log\left(\frac{1}{n}\Sigma_{i=1}^{n} 1/y_i^2\right)$

y_i denotes the results of the ith turn of a set of n simulated trials.

4 Optimization Procedure: Taguchi Method and Simulation Planning

The Taguchi method was originally developed for quality engineering in order to evaluate and improve robustness of products, tolerance specification, and quality management of a production process [18]. It does not draw upon complicated probability or statistical analysis. The methodology can be applied to our problem, which requires kinematic parameter optimization through simulation. With this method, an optimized solution can be obtained by design of experiments, which normally demands complicated mathematical expansion in the theoretical approach.

The Taguchi method divides the independent variables into controllable factors and noise factors. Controllable factors can be maintained to a desired value while noise factors may not be controlled. The Taguchi method can realize a robust design, which can maintain high performance as well as insensitivity to noise factors. In this section, we apply the Taguchi method in designing the experiments (or in this case the simulations) for maximizing the workspace and the mean stiffness of the suggested parallel mechanism. Under the framework of the Taguchi method [18], the basic steps for designing an experiment or simulation are as follows.

A. Identifying the objectives: In the first step of the Taguchi method, identifying a specific objective is important because it determines the objective function and influences the classification of variables into controllable factors and noise factors. The stiffness of the planar 2-DOF parallel manipulator of our study was related to the lengths of the links and the installed position of the actuators. Therefore, the objective is to examine the relationship among the workspace, the mean stiffness, and the kinematic parameter level.

B. Determining the objective function: The Taguchi method classifies the objective function into one of three types: nominal-the-best, smaller-the-better, and larger-the-better (see Table 1). The objective function in our case was the sum of the workspace and mean stiffness of the manipulator, and it was a larger-the-better problem.

C. Selecting the controllable factors and noise factors: The factors to be tested for their influence on the objective function are selected. This procedure determines which orthogonal array should be used according to the selected controllable and noise factors.

The length of links and the position of actuators were set as the controllable factors and the external forces exerted on the platform of the manipulator were set as the noise factor in this study. After selecting the factors, their desired number of levels was determined.

If the number of levels was set to two, only the influence of the selected factors could be investigated by response analysis, which will be showed later. If the number of levels was set to three, the influence and the

Table 2 Levels of controllable and noise factors of first stage simulation

	Controllable factor	Level 1 (mm)	Level 2 (mm)	Level 3 (mm)
A	l_{11}	224	280	336
B	l_{21}	224	280	336
C	l_{31}	224	280	336
D	l_{12}	224	280	336
E	l_{22}	224	280	336
F	B_{1x}	−240	−300	−360
G	B_{1y}	42	0	−42
H	B_{2x}	240	300	360
I	B_{2y}	42	0	−42
J	B_{3x}	120	150	180
K	B_{3y}	378	420	462

	Noise factor	Level (N)
A	Force exerted on the platform	2.56

optimal level (not always) of the selected factors could be investigated simultaneously. Thus, we set the number of levels for the lengths of the links and positions of the actuators to be three. Levels of the controllable factors were varied so that they could have the same variation ratio. The level of a noise factor was only one because the output displacement, which is the inverse of the stiffness, was proportional to the force exerted on the platform. The physical values assigned in this paper are given in Table 2. We set the levels of the controllable factors based on the kinematic parameters of the original 2-DOF manipulator. The force exerted on the platform (2.56 N) was set to maximum to guarantee linearity of the spring torsion bar mounted on the actuator.

D. Selecting an orthogonal array: A full factorial simulation requires the testing of all combinations of the factor levels. However, orthogonal arrays can be used to produce smaller but less costly simulations because it offers influence of each variable from least number of test times. There are several orthogonal arrays according to the combination of the level and the number of variables. It should be noticed that not all combinations exist. Therefore, we should select the orthogonal array, which has the most similar combination among the combinations that satisfy minimum requirement (that is level, number of variables). In this study, we used an L_{27} (3^{13}) orthogonal array. From the orthogonal array, first 11 columns are used and last two columns are ignored [18]. Mainly, in a full factorial simulation, $3^{11}=177{,}147$ simulations involving 11 factors at three levels are required. Applying the L_{27} (3^{13}) orthogonal array, only 27 simulations need to be carried out (for details about the L_{27} (3^{13}) orthogonal array, see Table 6 in the Appendix).

E. Simulations and analysis: Simulation and analysis are developed in the planning and design stages. The analysis stage of the simulation relates to the calculations that convert raw data into the representative signal-to-noise ratio (S/N ratio). As a measurement tool for determining robustness, the S/N ratio is an essential factor in the optimization of design parameters.

By representing the impact of noise factors on the process or product as the denominator, the S/N ratio can be adopted as the index of how well the system performs regardless of the noise effects. Analysis also includes the determination of the most important controllable factors, which can maximize the S/N ratio, and the selection of their optimal levels. Index to be optimized is defined as follows:

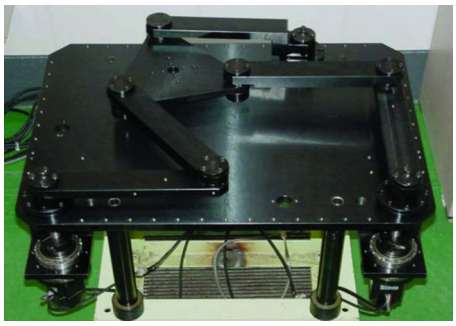

Fig. 4 Picture of the planar 2-DOF parallel manipulator with original dimension

$$I_{\text{output}} = w_1 \frac{A_{\text{act}}}{A_{\text{ori}}} + w_2 \frac{S_{\text{act}}}{S_{\text{ori}}}$$

$$\text{subject to } A_{\text{act}} > 0.4A_{\text{ori}} \tag{23}$$

where w_1 and w_2 are weight factors for the workspace and the mean stiffness. A_{ori} is the workspace area with the original parameter set-up, whereas A_{act} is the workspace area with the parameter of each simulation set-up. The workspace area $A(=M/n^2\times 100)$ is computed by counting points M in the total grid (n by n matrix), which satisfies inverse kinematic constraints. S_{ori} is the mean stiffness with the original parameter set-up, whereas the S_{act} is the mean stiffness with the parameter of each simulation set-up. The mean stiffness $S(=360M/f\Sigma_{j=1}^{M}\Sigma_{i=1}^{360}d_{ji})$ is a reciprocal of an average displacement. The average displacement is obtained by averaging displacements of all points of the workspace when the external force f is applied in all directions (360 deg). d_{ji} is displacement, where i and j indicate degree and computation point in the workspace, respectively. This index is a unique input value of the S/N ratio and it can be used directly as the S/N ratio. In the case of the workspace, there is a constraint to prevent the workspace from decreasing below the specified area.

5 Response Analysis

The manufactured planar 2-DOF parallel manipulator is shown in Fig. 4 with the original dimensions, which are listed in Table 3. The lengths of five links were equal, and the third actuator was mounted a little apart from the center of the other actuators in the horizontal direction.

The number of design variables that had more influence than the other design values was found by response analysis of the Taguchi method. The design variables of the planar 2-DOF parallel manipulator included the length of the links and the position of the actuating joints. With the result of 27 simulations, we averaged S/N ratios for each level of the controllable factors, which were calculated based on the orthogonal array. For example, Eq. (24) represents the computation of the average S/N ratio of controllable factor A.

Table 3 Original dimensions of the planar parallel manipulator

Legend	Meaning	Value (mm)
d	Dimension of a side of tool platform	215
l	Length of link	280
B_1	Position of first actuating joint	(−300, 0)
B_2	Position of second actuating joint	(300, 0)
B_3	Position of third actuating joint	(150, 420)

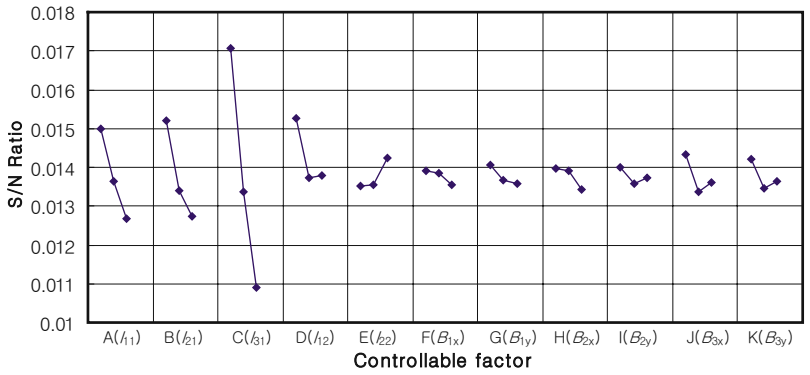

Fig. 5 Response graph: average S/N ratios for the eleven controllable factors

$$\eta(\text{level } A_1) = \frac{\sum_{i=1}^{9} A_{1i}}{9}$$

$$\eta(\text{level } A_2) = \frac{\sum_{i=1}^{9} A_{2i}}{9}$$

$$\eta(\text{level } A_3) = \frac{\sum_{i=1}^{9} A_{3i}}{9} \tag{24}$$

Figure 5 shows the response analysis of the first stage simulation. It shows the average S/N ratios of each controllable factor in three levels when weight w_1 equals w_2 ($w_1 : w_2 = 1:1$). Each alphabet denotes the corresponding kinematic parameter, as shown in the Table 2. Figure 5 indicates that the first four controllable factors, the lengths of l_{11}, l_{21}, l_{31}, and l_{12}, have stronger effects on the optimization index, whereas l_{22} and the position of actuators have little influence.

The influence of the average S/N ratio of the first four controllable factors is obvious. As the lengths of l_{11}, l_{21}, l_{31}, and l_{12} become longer, the workspace itself increases, naturally. However, the mean value of stiffness decreases when the lengths of the linkages increases. With respect to this point, the rate of decrease of mean stiffness is greater than the rate of increase of the workspace. Therefore, the average S/N ratio becomes smaller, as the lengths of l_{11}, l_{21}, l_{31}, and l_{12} increases.

Based on the result of the first simulation, we conducted an additional simulation with the four controllable factors l_{11}, l_{21}, l_{31}, and l_{12}. We applied the L_9 (3^4) orthogonal array in this simulation. For details of the L_9 (3^4) orthogonal array, see Table 7 in the Appendix.

The magnitude of the force exerted on the platform was the same as that of the first simulation. We applied smaller values for the levels of the three links l_{11}, l_{21}, l_{31} but applied a bigger value for the level of the link l_{12} than those of the first simulation. The bigger value has applied to the link l_{12} because the S/N ratio started to increase at the third level, and it is needed to maintain the minimum workspace constraint by applying bigger link length. In fact, at the second simulation, the S/N ratio of the link l_{12} increased as the level increases.

Figure 6 shows the result of the response analysis about the average S/N ratios with respect to the four controllable factors, which are the lengths of four links l_{11}, l_{21}, l_{31}, and l_{12}. Among the four links, the third link l_{31} was the most influential factor. The average S/N ratios for the first three controllable factors, the lengths of links l_{11}, l_{21}, l_{31}, seemed to be similar to each other but the fourth controllable factor, the length of link l_{12}, was not similar to the average S/N ratios of the other three controllable factors. Links l_{11}, l_{21}, l_{31} were connected directly on actuators but link l_{12} was connected to link l_{11} indirectly.

6 Simulation Results and Discussion

The optimization procedure yielded new kinematic parameter groups (see Table 4). The new parameter group gave better performance than the original kinematic parameter group did with respect to the workspace and mean stiffness of the planar 2-DOF parallel manipulator.

The results of the simulation in the second stage are suggested in Table 5. In the results, the champion (quasi-optimal) group and the eighth group improved the performance of the manipulator by over 127% and 80%, respectively. The champion group showed distinctively high mean stiffness, and the eighth group showed high mean stiffness without much loss of the workspace. The detailed performance of each kinematic parameter group is depicted in Table 5, and the workspace and the stiffness of each case are depicted in Fig. 7. Figure 7 shows the workspace and the

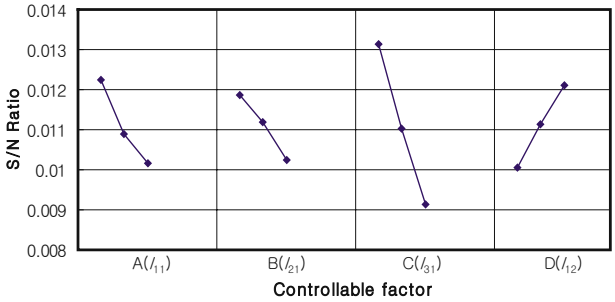

Fig. 6 Response graph: average S/N ratios for the four controllable factors

Table 4 Levels of controllable and noise factors of the second stage simulation

	Controllable factor	Level 1 (mm)	Level 2 (mm)	Level 3 (mm)
A	l_{11}	150	187	224
B	l_{21}	150	187	224
C	l_{31}	150	187	224
D	l_{12}	336	420	504
	Noise factor		Level (N)	
A	Force exerted on the platform		2.56	

Table 5 Result of the second stage simulation

Test No.	Controllable factors 1	2	3	4	Output ($I_{output}/I_{original}$)	Link length (mm) l_{11}	l_{21}	l_{31}	l_{12}	Workspace (m^2)	Mean stiffness (N/m)	Radius of gyration (m)
1	1	1	1	1	1.769	150	150	150	336	0.049	174.709	0.548
2	1	2	2	2	1.656	150	187	187	420	0.062	154.268	0.557
3	1	3	3	3	1.419	150	224	224	504	0.057	129.651	0.571
4	2	1	2	3	1.635	187	150	187	504	0.054	167.478	0.558
5	2	2	3	1	1.246	187	187	224	336	0.074	106.266	0.556
6	2	3	1	2	1.671	187	224	150	420	0.072	158.413	0.554
7	3	1	3	2	1.353	187	150	224	420	0.079	117.588	0.557
8	3	2	1	3	1.805	224	187	150	504	0.074	175.782	0.558
9	3	3	2	1	1.273	224	224	187	336	0.080	119.014	0.556
[a]	1	1	1	3	2.273	150	150	150	504	0.047	246.705	0.555

[a]Denotes champion group obtained from the second response analysis.

stiffness graph from the second stage simulation ($w_1:w_2=1:1$). The contours plotted inside the workspace represent the stiffness of the manipulator.

Mean stiffness is computed by averaging the stiffness of all points in the total workspace. As mentioned, the triangle and the connected lines in Fig. 7 constitute the corresponding kinematic structure. A circle, which is displayed as a dotted line, represents the radius of gyration. For convenience, the magnitude of the radius is scaled down by half. The radius of gyration is represented as below.

$$R_{\text{gyration}} = \sqrt{\frac{I}{A}}, \quad I = \int r^2 dA \tag{25}$$

where I is the second moment of inertia along the axis located in the center of an area and A is the workspace area. With the radius of gyration, we can investigate the workspace distribution around the centroidal axis of the workspace whether the workspace is distributed broadly or not.

The first group is composed of link parameters, which have first levels, and naturally its workspace is the smallest among the first eight groups. The radius of gyration is also the smallest among all the parameter groups, which means that the workspace is concentrated at the center of the area. The second group has a more broadly distributed workspace because of the longer links l_{21}, l_{31}, and l_{12} than those of the first group. The third group has link parameters of extreme values (level one or three) and thus, it nearly leads to the separation of the workspace into two parts. This result can be explained by the long radius of gyration, which comes from the scattered distribution of the workspace.

The fourth group has the same level of link l_{12} with the third group and middle level of links l_{11} and l_{31}. Because of the lengths of the links l_{11} and l_{31}, the fourth group has higher mean stiffness than the third group. The fifth group has the lowest mean stiffness whose levels of links l_{31} and l_{12} are opposite of those of the eighth group, which has the highest mean stiffness. The sixth group has a similar shape of workspace and radius of gyration to the fifth group, except for the relatively higher mean stiffness. The last three groups have similar combinations of link parameters, workspace, and radius of gyration. However, there are distinctive differences in the levels of links l_{31} and l_{12}. Only the eighth group has a lower level of link l_{31} and higher level of link l_{12}, which produce higher mean stiffness than those of the seventh and the ninth group.

The champion group (quasi-group denoted by * in Table 5 and Fig. 7) was obtained by taking the value of the control parameters with the highest S/N ratio in Table 5. It has incomparably high mean stiffness, which compensates the decrease in the area of the workspace. Actually, the workspace of the champion group is small and its geometrical shape is not so usable. The champion group, however, suggests that it is possible to produce a kinematic

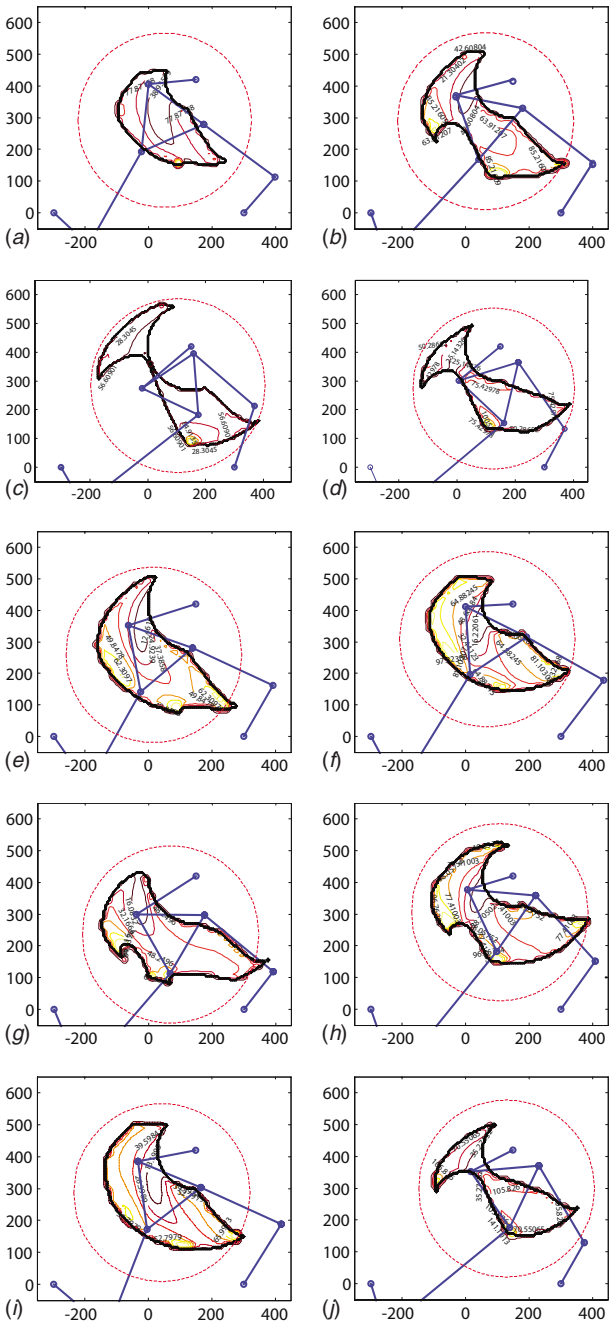

Fig. 7 Workspace and stiffness graph as a result of the second stage experiment

Table 6 L_{27} (3^{13}) orthogonal array

	Controllable factor												
Test No.	1	2	3	4	5	6	7	8	9	10	11	12	13
1	1	1	1	1	1	1	1	1	1	1	1	1	1
2	1	1	1	1	2	2	2	2	2	2	2	2	2
3	1	1	1	1	3	3	3	3	3	3	3	3	3
4	1	2	2	2	1	1	1	2	2	2	3	3	3
5	1	2	2	2	2	2	2	3	3	3	1	1	1
6	1	2	2	2	3	3	3	1	1	1	2	2	2
7	1	3	3	3	1	1	1	3	3	3	2	2	2
8	1	3	3	3	2	2	2	1	1	1	3	3	3
9	1	3	3	3	3	3	3	2	2	2	1	1	1
10	2	1	2	3	1	2	3	1	2	3	1	2	3
11	2	1	2	3	2	3	1	2	3	1	2	3	1
12	2	1	2	3	3	1	2	3	1	2	3	1	2
13	2	2	3	1	1	2	3	2	3	1	3	1	2
14	2	2	3	1	2	3	1	3	1	2	1	2	3
15	2	2	3	1	3	1	2	1	2	3	2	3	1
16	2	3	1	2	1	2	3	3	1	2	2	3	1
17	2	3	1	2	2	3	1	1	2	3	3	1	2
18	2	3	1	2	3	1	2	2	3	1	1	2	3
19	3	1	3	2	1	3	2	1	3	2	1	3	2
20	3	1	3	2	2	1	3	2	1	3	2	1	3
21	3	1	3	2	3	2	1	3	2	1	3	2	1
22	3	2	1	3	1	3	2	2	1	3	3	2	1
23	3	2	1	3	2	1	3	3	2	1	1	3	2
24	3	2	1	3	3	2	1	1	3	2	2	1	3
25	3	3	2	1	1	3	2	3	2	1	2	1	3
26	3	3	2	1	2	1	3	1	3	2	3	2	1
27	3	3	2	1	3	2	1	2	1	3	1	3	2

parameter group, which has a better performance by combining the value of the control parameters with the highest S/N ratio when the geometrical constraint given to the workspace.

The lengths of the linkages have stronger influence on the workspace and the mean stiffness than the other kinematic parameters such as the position of the actuators. By analyzing the results, the tendency about the relationship of the link length to workspace and mean stiffness of the planar 2-DOF parallel manipulator can be observed.

(1) As the length of the link connected directly to each actuator becomes shorter, the more the mean stiffness is increased. Similarly, as the length of the link connected indirectly to each actuator becomes longer, the more the mean stiffness is increased. The result demonstrates the Lever law [11]. The force exerted on the center of the platform is transferred to the actuator through the link directly attached. The torque produced by the exerted force is decreased or increased in proportion to the length of the link. Therefore, a shorter link can produce higher stiffness.
(2) The shape of a workspace is related to the usable workspace defined by Liu et al. [10]. We evaluated the radius of gyration of each workspace to measure the distribution of the workspace. A small radius of gyration means that the workspace is distributed near the center of the workspace. The result shows that the long link contributes to a long radius of gyration and small usable workspace. In the case of the third group, the radius of gyration is longest, and the workspace is nearly divided into two parts, which means the workspace is less usable. Therefore, we should reduce the radius of gyration to ensure enough usable workspace.
(3) The amount of change in workspace and mean stiffness had relatively low sensitivity to the install positions of the three actuators based on the result of the first response analysis. Therefore, the actuators can be installed in near positions in the base frame to minimize the space needed to mount the manipulator.
(4) By adjusting link lengths, it is possible to organize a manipulator satisfying a variety of workspaces and mean stiffness without replacing actuators or changing the mount position of the actuators. The optimal kinematic parameter group is profitable for designing a manipulator that requires exceedingly high stiffness and not so large workspace such as a high precision-miniature part manufacturing machine tool. Also the eighth group is profitable for designing a manipulator that requires high stiffness and large workspace simultaneously such as a rapid prototyping machine tool.

With the observations mentioned above, it is possible to design an effective planar parallel manipulator, which has high stiffness as well as a relatively large workspace area.

7 Conclusions

We presented a kinematics parameter optimization that maximizes the workspace of the planar 2-DOF parallel manipulator as well as the mean stiffness inside the workspace.

Table 7 L_9 (3^4) orthogonal array

	Controllable factors			
Test No.	1	2	3	4
1	1	1	1	1
2	1	2	2	2
3	1	3	3	3
4	2	1	2	3
5	2	2	3	1
6	2	3	1	2
7	3	1	3	2
8	3	2	1	3
9	3	3	2	1

The Taguchi method was applied in this optimization to examine the relationship of each link and to separate relatively influential kinematic parameters. The Taguchi method was designed to simplify optimization procedures and to reduce the number of simulations at the cost of precision in finding the optimal solution. The optimization minimized the decrease of the workspace but maximized the increase of the mean stiffness of the manipulator. Kinematic analysis and stiffness analysis were employed in the optimization. Based on the results, we found a new kinematic parameter level group.

Using an orthogonal array, we reduced the number of simulations. Through the first response analysis, the number of experimental variables was reduced to separate the more influential controllable factors from the less influential ones in the optimization procedure. By additional simulations, the optimal kinematic parameter group was obtained. We also discussed the relationships among the link length, the workspace, and the mean stiffness. As a future work, the adjoint variable method can be applied in response analysis, which is desired when the dimensions of design variables are larger than the number of response functions such as a stiffness optimization of a spatial parallel mechanism.

Acknowledgment

This paper was supported by the second stage of the Brain Korea 21 Program of Seoul National University, by the research program 2010 of Kookmin University in Korea, and by the Seoul Research & Business Development Program (Grant No. 10583)

Nomenclature

- $\{B\}$ = base coordinate frame
- $\{T\}$ = tool coordinate frame
- x_t = position of center of platform based on $\{B\}$
- P_i = position of ith platform revolute joint based on $\{B\}$
- B_i = position of ith base revolute joint based on $\{B\}$
- S_i = position of ith revolute joint between links based on $\{B\}$
- q_i = angular position of ith joint ($i=1,\ldots,n$)
- q_r = angular position of actuation joints
- q_u = angular position of independent joints
- q_v = angular position of dependent joints
- l_{ij} = length of jth link of ith link branch
- d = length of a side of platform
- U = relocation matrix reassigning the order of independent and dependent joint vector into a ascending order
- V = selection matrix extracting actuation joint vector among all joint vectors
- g = constraint equation between three revolute joints
- J = Jacobian between velocity of platform and that of all joints
- G = constraint Jacobian
- τ_u = independent joint torques
- τ_r = actuated joint torques

Appendix

The L_{27} (3^{13}) and L_9 (3^4) orthogonal array are presented in Tables 6 and 7, respectively.

References

[1] Park, F. C., and Kim, J. W., 1999, "Singularity Analysis of Closed Kinematic Chain," ASME J. Mech. Des., **121**(1), pp. 32–38.
[2] Chakarov, D., 2004, "Study of the Antagonistic Stiffness of Parallel Manipulators With Actuation Redundancy," Mech. Mach. Theory, **39**, pp. 583–601.
[3] Kim, S., In, W., Yim, H., Jeong, J. I., Park, F. C., and Kim, J., 2007, "Stiffness Enhancement of a Redundantly Actuated Parallel Manipulator Using Internal Preload: Application to a 2-d.o.f Parallel Mechanism," Asian Symposium for Precision Engineering and Nanotechnology.
[4] Laycock, S. D., and Day, A. M., 2003, "Recent Developments and Applications of Haptic Devices," Comput. Graph. Forum, **22**, pp. 117–132.
[5] Birglen, L., Gosselin, C., Pouliot, N., Monsarrat, B., and Laliberté, T., 2002, "SHaDe, A New 3-DOF Haptic Device," IEEE Trans. Rob. Autom., **18**(2), pp. 166–175.
[6] Siva, K. V., Dumbreck, A. A., Fischer, P. J., and Abel, E., 1988, "Development of a General Purpose Hand Controller for Advanced Teleoperation," Proceedings of the International Symposium on Teleoperation and Control, pp. 277–290.
[7] Xu, Q., and Li, Y., 2006, "Stiffness Optimization of a 3-DOF Parallel Kinematic Machine Using Particle Swarm Optimization," Proceedings of the IEEE, International Conference on Robotics and Biomimetics, pp.1169–1174.
[8] Xu, Q., and Li, Y., 2008, "An Investigation on Mobility and Stiffness of a 3-DOF Translational Parallel Manipulator via Screw Theory," Rob. Comput.-Integr. Manufact., **24**(3), pp. 402–414.
[9] Lee, J. H., Yi, B. J., Oh, S. R., and Suh, I. H., 1998, "Optimal Design of a Five-Bar Finger With Redundant Actuation," Proceedings of the IEEE, International Conference on Robotics and Automation, pp. 2068–2074.
[10] Liu, X.-J., Wang, J., and Pritschow, G., 2006, "Kinematics, Singularity and Workspace of Planar 5R Symmetrical Parallel Mechanisms," Mech. Mach. Theory, **41**, pp. 145–169.
[11] Liu, X.-J., Wang, J., and Pritschow, G., 2006, "Performance Atlases and Optimum Design of Planar 5R Symmetrical Parallel Mechanisms," Mech. Mach. Theory, **41**, pp. 119–144.
[12] Lee, Y. H., Han, Y., Iurascu, C. C., and Park, F. C., 2002, "Simulation-Based Actuator Selection for Redundantly Actuated Robot Mechanisms," J. Rob. Syst., **19**(8), pp. 379–390.
[13] Lee, K. H., and Kim, J., 2000, "Controller Gain Tuning of a Simultaneous Multi-Axis PID Control System Using the Taguchi Method," Control Engineering Practice, **8**(8), pp. 949–958.
[14] Rout, B. K., and Mittal, R. K., 2008, "Parametric Design Optimization of 2-DOF R-R Planar Manipulator—A Design of Experiment Approach," Rob. Comput.-Integr. Manufact., **24**, pp. 239–248.
[15] Garg, V., Nokleby, S. B., and Carretero, J. A., 2009, "Wrench Capability Analysis of Redundantly Actuated Spatial Parallel Manipulators," Mech. Mach. Theory, **44**, pp. 1070–1081.
[16] Nokleby, S. B., Fisher, R., Podhorodeski, R. P., and Firmani, F., 2005, "Force Capabilities of Redundantly-Actuated Parallel Manipulators," Mech. Mach. Theory, **40**, pp. 578–599.
[17] Gosselin, C., and Angeles, J., 1990, "Singularity Analysis of Closed-Loop Kinematic Chains," IEEE Trans. Rob. Autom., **6**(3), pp. 281–290.
[18] Peace, G. S., 1993, *Taguchi Methods—A Hands On Approach*, Addison-Wesley, New York.